Reaction Chemistry & Engineering

ROYAL SOCIETY OF CHEMISTRY

PAPER

View Article Online
View Journal | View Issue

Cite this: *React. Chem. Eng.*, 2020, 5, 1450

Activation of homogenous polyolefin catalysis with a machine-assisted reactor laboratory-in-a-box (μAIR-LAB)

Benjamin A. Rizkin and Ryan L. Hartman *

Traditionally catalysis research and development has been limited to large purpose-built labs, requiring years of planning and implementation before the first molecules were even examined. However, recent developments in microfluidics, robotics, system miniaturization and machine intelligence allow the decoupling of research from multi-million dollar purpose-built facilities. Additionally this scaling-down of research has significant benefits for the environment, development timelines and researcher workload. In this publication we demonstrate the construction of a microfluidic catalysis research platform contained within a standard hard-sided case measuring just 0.73 m^2, consuming under 100 W of power, and generating 66.7 μL of chemical waste per min. The system integrates a purpose-built microreactor with hot-swappable chuck, vacuum enclosure, manifolds, pumps, robotic autosampling, open-source controls and thermographic performance analysis. The system was used to investigate nine chemically different activators for a zirconocene-catalyzed α-olefin polymerization through efficient experimentation and automated transfer learning ML-based data interpretation. The contributions of different chemical structures to catalytic productivity were analyzed. Conclusions made include those regarding co-catalyst chemistry and probable operating conditions. This work demonstrates that a compact flow-based microfluidic platform can screen exothermic catalytic reactions and interpret the results using machine intelligence.

Received 8th April 2020,
Accepted 18th June 2020

DOI: 10.1039/d0re00139b

rsc.li/reaction-engineering

Introduction

Over the last century developments in polymer science have changed numerous aspects of our lives. Originally just academic curiosities, scientists and engineers optimized these fascinating molecules to fit needs in almost every corner of our society from household goods to medical implants. A class of polymers which has been of special interest are poly(olefins), chains of alkenes with highly tuneable microstructures that can be transformed into a wide range of practical materials. Currently poly(olefins) are an industry worth over $200 billion per year developing 170 million tons of product, one of the largest volume commodity materials in the world.[1] Research into poly(olefin) catalysis continues at a rapid pace as the drive for more highly tuned properties and greener materials continues.[2,3] However, polymerization reactions are relatively more difficult to study as opposed to some other forms of organic transformations due to the complex reaction mechanisms, sensitivity to impurities and non-trivial chain growth kinetics. The theme of microfluidics and a drive towards automation and miniaturization have influenced the methodology of this study as they offer ways to overcome these difficulties. This study offers insight into how systems for the investigation of catalytic polymerizations can be miniaturized, providing faster and greater insight into molecular behaviour than was previously possible. Additionally benefits exist in process safety, environmental footprint and the time to actionable data. Finally the presented system is unique in the sense that it allows one to decouple catalytic research from a purpose-built laboratory offering new opportunities and research directions for future works.

Metallocene catalysis

Metallocene catalysts, typically a group IVB organometallic compound, are paired with a transition metal activator, often borate or aluminate compounds. The exact structure of the catalyst and the composition of the activator can have a profound effect on the chemical and morphological structure of the final polymer.[4] There have been many studies on the topic as the applicability of metallocene and Ziegler–Natta (supported metallocene) catalysis to the poly(olefin) market has large economic implications leading to much academic and industrial interest. Recent studies have focused on investigating polymer properties,[5] catalyst preparation,[6] active

New York University, Department of Chemical and Biomolecular Engineering, 6 MetroTech Center, Brooklyn NY, 11201, USA. E-mail: ryan.hartman@nyu.edu

site analysis,[7] stereoselectivity,[8] regioselectivity,[9] fundamental properties through molecular simulations[10,11] and many other areas of interest while still presenting challenges to researchers.[12] Also there have been a significant amount of studies on the chemistry, behaviour and performance of different co-catalysts with a review by Chen and Marks summarizing many of the most important discoveries.[13] However, methodology for efficiently matching catalyst with cocatalysts based on performance characteristics is lacking as experimental batch techniques are time-consuming, expensive, and they generate significant quantities of chemical waste. In this study we aim to shed light on how flow-based microfluidics combined with high throughput experimentation can be used for this important challenge. Through better understanding these complex catalytic systems it becomes possible to design catalysts which are active with certain monomers, better tune the resultant polymers, and design systems for optimistic environmental and technoeconomic goals.

Flow chemistry and microfluidics

Two fields which are driving progress in scientific discovery in catalysis are flow chemistry and microfluidics. By performing reactions in flow it becomes possible to exhibit better control over the reaction, produce more homogeneous products and enhancing process economics.[14] From an industrial perspective, this is important because the market value of polymers is directly driven by their consistency and properties. Additionally flow reactors are easier to scale by running multiple reactions in parallel and reducing feedback loops and impurities.[15] From an academic perspective however, flow chemistry is interesting because it allows for elucidation of fundamental parameters of interest quickly and efficiently without relying on time-consuming batch experimentation and enables the integration of robust automation.[16] Kinetic information can be obtained using *in situ* methodology, reducing both the time-to-discovery and material needs over batch systems.[17,18] Additionally, microfluidics allows for tight control over the reaction environment by decreasing the volume of the medium; by miniaturizing the reaction surface forces begin to outweigh body forces, allowing for preferential control over heat and mass transport. Overall the adoption of microfluidic technology assists not only with the physical and chemical optimization of the system, but also allows studies to be performed using milli-to-nano gram amounts of reagents, significantly decreasing the environmental footprint of research.[19]

Recently microreactors have been employed extensively in polymer synthesis and investigation. Notable investigations performed recently include the application of microreactor technology to ATRP, RAFT, anionic, ROP, click BCP, FRP and Ziegler–Natta polymerization systems.[16,20–31] Overviews of application of microreactors in polymer synthesis have been published recently by Tonhauser *et al.* and Su *et al.* and offer a broad overview of developments in the field.[19,32] It should however be noted that applying microreactors to the flow synthesis of polymers is not without challenges. The primary challenge is the blockage of the microchannels, which can either completely stop flow or significantly change the residence time distribution (RTD) within the reactor.[33] As the RTD within the reactor changes the reaction rate and morphology of the forming polymer will also change as various quanta of fluid spend more or less time in the reaction channel. This phenomenon has been observed in the work of Reis *et al.* who investigated the effects of residence times and RTDs in continuous polymerizations and Song *et al.* who investigated the influence of mixing on polymerization of acrylamide in capillary microreactors.[31,34] Additionally researchers have employed droplet flow microfluidics, a flow regime where slugs of liquid are separated by either an inert liquid or a gas, to achieve higher levels of mixing and control within the polymerization reaction.[34–36] Overall, microreactors provide an interesting new platform for the synthesis of polymers both in the laboratory and for specialty application in industry, with a demonstrated track record of success over the last few decades.

High throughput screening, artificial intelligence and machine learning

In addition to flow chemistry and microfluidics, faster and more labour efficient research has also been enabled by the implementation of high throughput (HT) screening, machine learning (ML) and artificial intelligence (AI) with chemical systems. By taking labour away from the chemist and putting it in the hands of a "robot" it becomes possible to decouple the laborious tasks of mixing reagents, switching chemicals, measuring input/output (I/O) pairs of the experiment and collecting process data, enabling the researcher to focus his or her time on tasks not amenable to automation. In recent years automation and HT screening has been employed extensively for materials discovery, process optimization and polymer research both in academia and industry.[37–39] In 2009 Busico *et al.* used HT screening with miniaturized parallel reactors to quickly screen heterogeneous olefin polymerization catalysts.[40] Their system employed a commercial Symyx PPR® setup with parallel mini-reactors with both online and offline analytics to quickly screen the polymerization rate and catalytic productivity of hafnocene catalysts.[40] Also Chammingkwan *et al.* used HT screening for the design of support materials for heterogeneous olefin polymerization catalysts, synthesizing 24 magnesium ethoxide samples and drawing conclusions based on principle component analysis, leading to a better understanding of these support materials.[41] Other relevant works include the research of Schubert *et al.* who used HT experimentation to study atom transfer radial polymerizations.[42,43] Recent work employing HT screening for metallocene catalysis reaction design includes quantitative measurements of regioselectivity

by Vittoria *et al.*[44] Also HT automated experimentation has been paired with combinatorial methods to quickly and efficiently design, synthesize and screen large libraries of potential catalyst molecules quickly and efficiently.[2] Finally the recent work of Rubens and Junkers *et al.* has employed highly autonomous flow reactors integrated with size exclusion chromatography (SEC) and nuclear magnetic resonance (NMR) to optimize polymerization reactions for particular characteristics including molecular weight.[45] Their work has shown the applicability of intelligently designed and implemented systems to replace tedious experimentation with novel automated methods.[46] Overall automation and HT experimentation and screening are crucial tools for catalysis and especially polymer research in the 21st century.

Recently the prevalence and academic/industrial usefulness of ML and AI to polymer design and catalysis challenges have been expanding, particularly when coupled with on-line or *in situ* analytics for fast decision making. AI enables for both the separation of the practical operation of a system from knowledge of the full mathematical model while also giving scientists and engineers the ability to extract more information from fewer experiments. At the same time, ML enables machines to learn about the performance and operational characteristics of chemical systems in real time, building the aforementioned models either without or with minimal human interaction (unsupervised *vs.* supervised learning). In recent years ML has been applied quite extensively to polymer design both from a fundamental chemistry aspect and from the perspective of experimental design.[47–54] At the same time online analytics have been integrated extensively with polymerization systems of all kinds with reviews and relevant articles being readily available in the literature.[55–61] Of particular interest are approaches using heat balances, as the heat of a reaction can be tied directly to the activity of the catalyst while also being easy to measure experimentally. This approach has been used by ref. 60–64 with critical analysis and comparisons of methodologies being presented by ref. 60, 65 and 66. The heat balance is also aided by the application of microfluidics where the flow of heat into and out of the system can be precisely monitored and calculated. By ensuring laminar flow with minimal axial mixing, each quanta of fluid can be treated as a separate heat balance. With the reduction of body forces heat transfer within the medium can also be well accounted for.[59,67] Finally by constructing the system out of infrared transparent materials, the heat produced by the reaction can be quantified and analysed in real time using thermography. The use of infrared thermography and temperature stability in a comparable system has been previously investigated.[68] By combining online analytics with ML it becomes possible to analyse complex polymerization chemistries in real time. By further combining the models with either informed interpretation or AI analysis it becomes possible to make actionable conclusions based on the data. Overall the combination of online polymer analytics with ML and AI data interpretation is a powerful new tool for research.

Methodology

In the present study, an integrated microfluidic system was designed and constructed for the purpose of analysing zirconocene alpha(olefin) polymerization reactions in an automated fashion. The system was integrated into a Pelican® transport case for easily mobility both inside the lab and to other environments. A picture of the system with all major components labelled can be seen in Fig. 1 below and a schematic representation can be seen in Fig. 3. As green catalysis research has been becoming more and more relevant to different industries while also becoming more proprietary, we have identified mobility and modularity as crucial design factors. The philosophy being that in addition to investigating catalysts and activators in our own lab the system can be brought over to other laboratories, including of both academic and industrial partners, or remotely deployed in chemical manufacturing sites. Additionally, in the future, the system can be moved closer to point-of-use for large spectroscopic instruments like high frequency NMRs or synchrotrons. The reactor platform is designed in such a way that the microreactor can be easily substituted for a millifluidic or other reactor. The enclosure contains features that enable a modular approach to reactor selection and implementation.

Reactor lab-in-a-box (μAIR-LAB)

Support infrastructure/power supplies. The first aspect of the case is an integrated power and controls management strategy. The design criteria include maximum portability and ease of adaptation, so it was critical to maintain minimal connections to the outside world. The box is only connected with a single power cable (110 V, 15 A), which supplies a protected power strip. The power strip is then in turn connected to a series of transformers and DC rectifiers to the various low-voltage electronics in the box. The total power draw at standby is ~20 watts and while operating is ~75 watts (as measured by a Sherpa® AC100 power inverter), enabling power to easily be fed from a battery enabling off-grid operation. A single Li-ion 18650 cell would provide between 5–10 minutes of use. Aside from a nitrogen supply and vacuum pump the system is entirely self-contained.

Control panel. A control panel offers the user a quick overview of the current status of the box including voltages on the various rails and the status of various components. This is necessary to ensure safe and informed operation. The control panel also includes a keyboard and mouse for interacting with the control software.

Control computer and interface. A laptop computer (Lenovo Flex 5, Intel i7, 16 GB RAM) is included for process control. The computer is running a combination of LabVIEW® 2019, MATLAB® R2019A and proprietary control software/libraries for the various integrated pumps, manifolds, IR camera, robotic arm, *etc.* The laptop also provides remote access and configuration ability along with

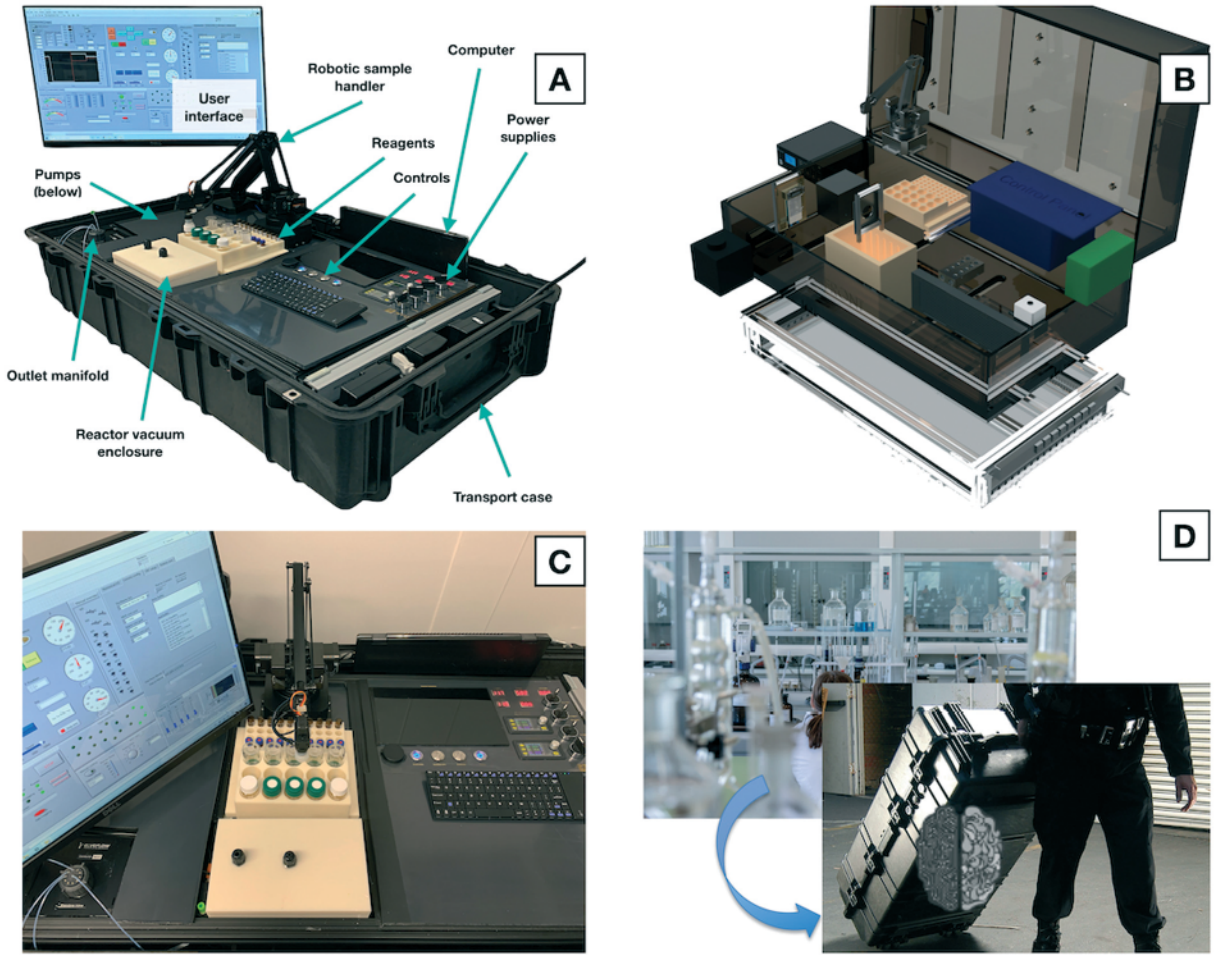

Fig. 1 (A) Overview of the μAIR-LAB system showing the box with all major components labelled. The system consists of a transport case with internal framework constructed of 1″ T-slotted framing. Into the framework are built power supplies, pumps, manifolds, a reagent holder, robotic arm and microreactor enclosure. The system is highly compact and portable while offering large flexibility for different types of chemical studies. (B) Blown up CAD rendering showing how all the components fit into the case. (C) A vertical view highlighting the reagent handling system and robotic arm. (D) Demonstration of how the technology presented here can transition the work traditionally done in a purpose-built laboratory to a portable system [photo of man rolling case courtesy of, and used with permission from, Pelican Products, Inc.].

having enough processing power for data analysis and visualization.

Reagent storage. The central premise of a high-throughput experimental station is the ability to store and utilize numerous reagent combinations automatically and safely. For this reason, we have fabricated a custom 3D printed reagent shelf with slots for standard vials. The slots offer either the ability to hold the reagent with the septum facing up and the robotic arm piercing it with a needle, or the ability to insert needles form the bottom and have the robotic arm place the vials onto them. The first scenario is more useful when a lower residence volume is desired, as there is no need for an input manifold between the needle and reactor. The second case is used when cross-contamination between the samples is a critical concern. Chemical waste is collected in a 250 mL container equipped with a 1/4-28 connection for chemically-resistant PTFE tubing. The container can be equipped with a carbon filter or exhaust tube to eliminate potential pressure buildup. Overall the reagent storage and management solution is designed in such a way as to maximize the flexibility of the system for future studies.

Microreactor and enclosure. The system in question relies on a microreactor for fast and efficient experimentation with the chip lying at the centre of the box and being interconnected with the various pumps and manifolds. The microreactor has two parallel feed channels used to establish laminar flow and heat/cool the reagents as necessary. These channels are followed by a micromixer section consisting of a series of radiused segments to encourage fluid mixing. The total volume of the micromixer section was 60 μL, having a width of 1 mm and a depth of 2 mm. The micromixer segment encourages fast contact between the two phases, reducing the measured effects of mass transport and ensuring that the reaction runs in a reaction rate limited regime instead of a transport limited one. The chip is fabricated on a photopolymerization 3D printer (Objet® 3D) and is bound to an IR transparent material (PolyIR® 1) for

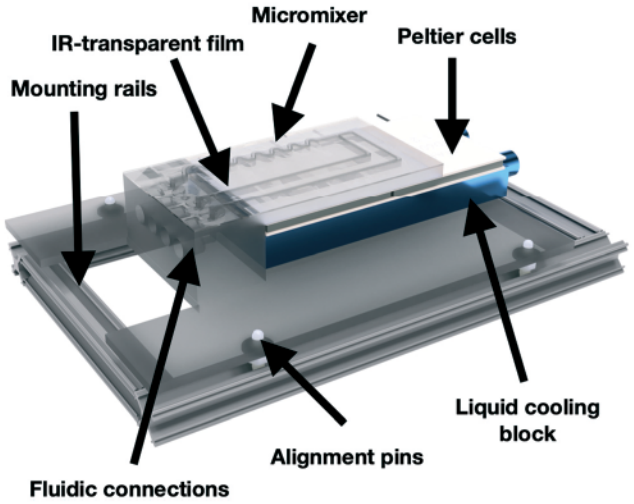

Fig. 2 Overview of the microreactor used for the current study showing the mounting rails, reactor chip and Peltier modules. The reactor consists of two flow channels and a micromixer section with an integrated chuck for fluidic interfaces.

analysis by a thermal camera. The chip can then be connected to two Peltier thermoelectric modules (Marlow® TR060-6.5-40 L) and a liquid circulation water block. The entire assembly is then bolted to miniature T-slotted framing which slots into the 3D-printed reactor enclosure. An overview of the reactor chip and mounting rails can be seen in Fig. 2. The reactor enclosure provides a passthroughs for the various fluidic tubes and wires while maintaining a vacuum to prevent IR interference and heat loss. Overall this reactor fabrication methodology allows for maximal flexibility when redesigning reactors for different experiments and minimizes the cost and labour that go into each chip.

While it would also be possible to use millifluidic reactors which are less prone to clogging for the study, however there are some disadvantages compared to microsystems. First, dispersion plays a role in these systems. To adequately quantify the catalytic system it is necessary that the two reagent streams mix quickly and efficiently. This is easier to accomplish in microfluidics due to the balance between surface and body forces. Also the quantity of fluids necessary in a millifluidic system would be greater. This has an impact both on the feasibility of conducting experiments with minimal quantities reagents while also posing safety issues in case of runaway reactions. Finally, microfluidics allows for a more robust sampling of the exotherm due to the negation of inhomogeneity in the system, reducing the effect of gradients.

Infrared camera. A calibrated infrared camera (ICI® 9640P) is contained within the reactor enclosure and is used to analyse the heat produced in the reaction channel. Data from the camera is fed over USB back to the control laptop.

Liquid cooling system. Heat is either removed or supplied to the Peltier thermoelectric modules by a standard liquid cooling system consisting of a pump, 360 mm radiator and fans. Liquid is pumped from the pump reservoir to the liquid circulation block, through the radiator and back into the reservoir. The system can also be branched through a manifold to provide heat removal to future spectroscopic instruments or a high-power graphics card for tensor computing. All experiments performed in this study were held at ambient temperature of 22.90 °C.

Robotic arm. A robotic arm (UARM Swift Pro) is used to reconfigure the placement of the reagents on the shelf. The arm is integrated with the LabVIEW® control software which controls its movements through a pre-configured matrix of reagent locations. The arm includes an open-source Arduino® microcontroller which can be expanded with computer vision capabilities. Either a suction cup or gripper is used.

Reagent handling and pumps. Chemical handling is supplied by a set of manifolds (Cole-Parmer® EW-01356-17), dosing pumps (Cole-Parmer® EW-73120-38), a pressure driven pump (Elveflow® OB1) in a reconfigurable arrangement using standard 1/4-28 fittings. This enables maximum flexibility for performing different types of experiments and mixing various concentrations in real time. Using fluidic resistance the minimum achievable flowrate is 10 μL min^{-1} and the maximum is 2000 μL min^{-1}. This corresponds to a minimum residence time of 1.5 seconds and a maximum of ~5 minutes.

Enclosure. The entire setup is built onto a modular 1″ T-slotted framing chassis and is placed into a Pelican® transport case. This enables future expansion while also maintaining mobility and safety. All electrical and chemical components are physically separated except for the Peltier modules and IR camera and the case is made of thick polypropylene which is able to contain most leaks. The system can be operated in an open arrangement inside of a fume hood, or the top can be placed on the transport case and connected to local ventilation when a fume hood is not available. Finally, the case can be easily shipped or transported due to the small footprint and low weight, including by a UAV if necessary. Overall the system was designed for maximum flexibility and applicability to both this and future studies.

Materials

All reagents for the experiments with the exception of the catalyst were purchased from Sigma-Aldrich® in the purest form available. This included the activators, solvents and monomer. The catalyst was purchased from MCAT. Electromagnetic pumps, solenoids, 1/4-28 fittings, PTFE tubing, ferules and associated components were purchased from Cole-Parmer®. Peltier cells and the DC relay were purchased from Digikey®. Various generic liquid cooling components, tubing, wires and fittings were obtained through Amazon® and other vendors. The Pelican® case and computer were obtained through B&H® and all structural components were purchased through McMaster-Carr ®.

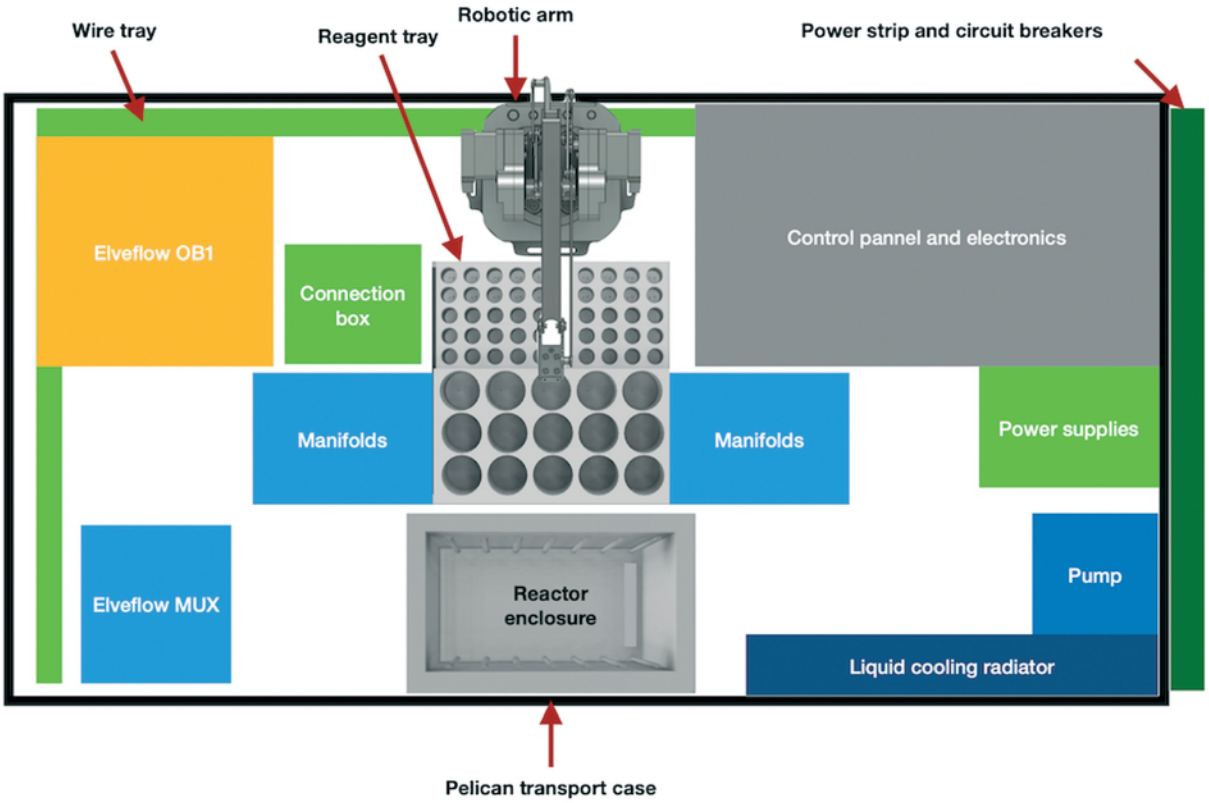

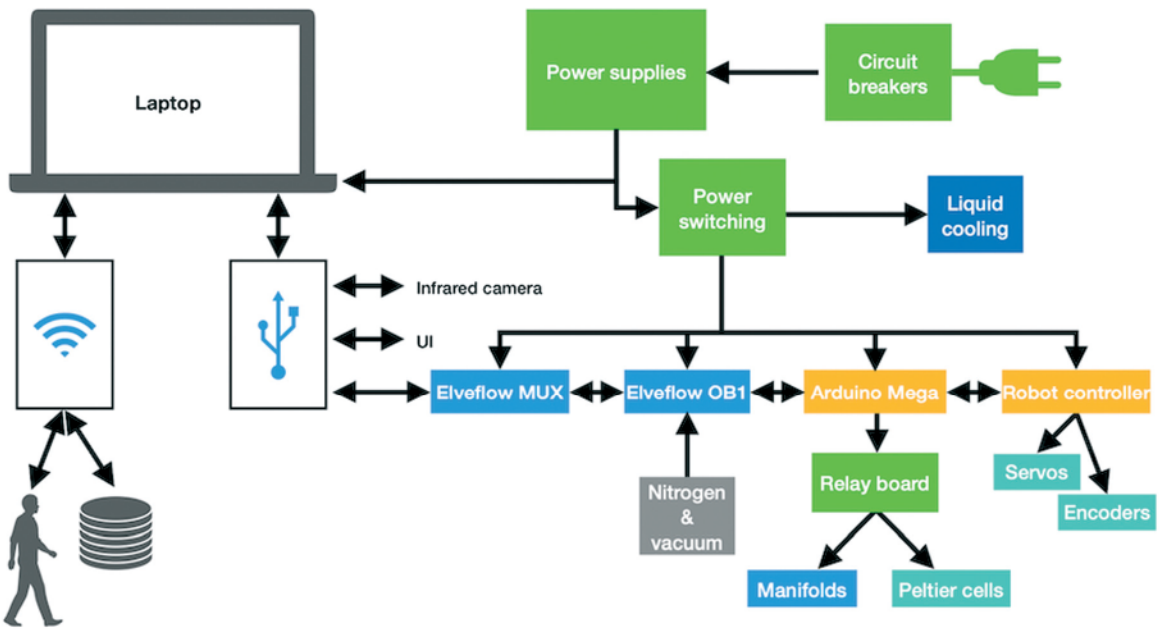

Fig. 3 (Top) Schematic workflow overview of the μAIR-LAB system highlighting the layout of components within the box including the pumps, manifolds, controls, power supplies and liquid cooling. (Bottom) Data and process flow diagram representing the various electronic sub-systems of the box and connections between them. The power switching includes two filtered 12 V supplies, a 5 V supply for the controls, and 3.3 and 24 volt supplies for future expansion.

Chemistry

A series of experiments was planned to investigate the effects of the various activators at different concentrations, holding all other parameters constant. A combination of nine activators was chosen based on the existing literature and on chemical intuition of the investigators in order to study

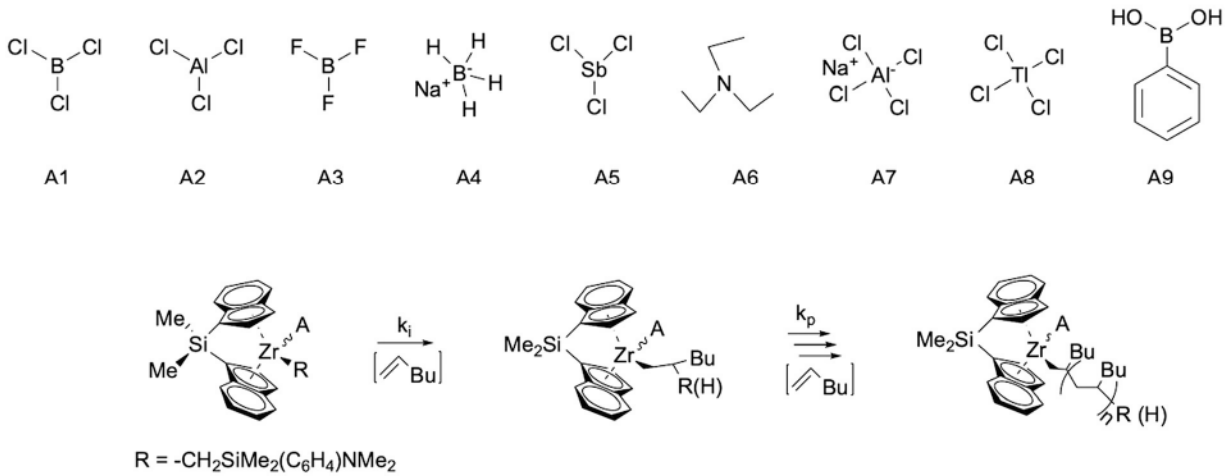

Scheme 1 (Top) The different activators used throughout this study, in order (A1) boron trichloride, (A2) aluminium chloride, (A3) boron trifluoride, (A4) sodium borohydride, (A5) antimony chloride, (A6) triethylamine, (A7) sodium tetrachloroaluminate, (A8) titanium chloride and (A9) phenylboronic acid. (Bottom) A simplified reaction pathway for a zirconocene-catalyzed polymerization reaction showing chain initiation and propagation with an activator (A).

performance with both known and unknown combinations (Scheme 1). The activators chosen included (**A1**) boron trichloride, (**A2**) aluminium chloride, (**A3**) boron trifluoride, (**A4**) sodium borohydride, (**A5**) antimony chloride, (**A6**) triethylamine, (**A7**) sodium tetrachloroaluminate, (**A8**) titanium chloride and (**A9**) phenylboronic acid (as a negative control). Experimental concentrations were chosen randomly for each activator between 1 and 7.5 mM with the goal of establishing a response profile while conserving catalyst and gather statistically valid data. All reagents were prepared in an inert environment glovebox operating at <0.3 PPM oxygen and <0.1 PPM water vapor. All activator and solvents were purchased in the highest purity form available from Sigma-Aldrich® and prepared vial serial dilution with a calibrated electronic micropipette. Note the compounds used in this study are hazardous chemicals and precautionary measures should be taken, such as use of proper personal protective equipment, as outlined in their respective safety data sheets. The risk of runaway reaction by an exothermic polymerization is also possible, though it is mitigated by the use of microfluidics.

Data was collected using an ICI® 9640P thermal camera contained in the experimental enclosure together with the reactor chip. Vacuum was applied to the enclosure as water vapor in the air would introduce noise into the data. Points for temperature measurement were selected from the frame of the camera and the exotherm automatically computed. Results were interpreted and saved into a database for further analysis. From this database catalytic activity was assessed by using a heat balance approach as the exotherm of polymerization per mole of monomer is known.

Next, the exotherms over the entire dataset were normalized (important for ANN training) and divided by the activator concentration in each trial to get a specific activity per mole of activator. This data was then combined with the trained ANN from our previous publication where numerous trials were run using the same catalyst and a tris(pentafluorophenyl)borane activator.[23] In previous publication conditions were selected to produce results comparable with previous studies using different techniques and by other laboratories using the same catalyst, ensuring the cross-validity of our microfluidic approach. Using transfer learning allows for the adaptation of existing ANN models to fit new datasets with a much smaller amount of data than the original training, reducing the chances of overfitting the network while providing a robust fit.†

Results and discussion

Upon completion of the schematic and practical design of the system all components were fabricated in-house using only standard tools. Construction of the system took approximately two weeks, including optimization and completion of the control code. When construction of the system was complete all sub-systems were commissioned which included performing pin assignments on the microcontroller, testing for parasitic current draw, leak testing and general workflow testing. After commissioning the entire system contained in the T-slot framing was lowered into the Pelican case and secured. Covers were then installed to ensure safe continuous operation.

Design considerations investigated and verified during commissioning included:

1) All components fit and secure inside the case framework as anticipated.

2) Sufficient distance and isolation is maintained between electrical components and chemical handling where hazards are present.

† The code and dataset analysed in this study can be found at: https://drive.google.com/drive/folders/17CZZ150Qg7zt-_vxOxMytUwIaRp3BbuY?usp=sharing.

3) Reagent holder aligns with robotic arm and sufficient range of motion is assured.

4) All fluidic connections are leak-free and hold both pressure and vacuum reliably.

5) All solenoids and pumps work as expected and interface with the control software without delay.

6) Air is bled from the liquid cooling loop and there is sufficient flow.

7) Reactor can be maintained in the desired environment thermally and atmospherically.

8) Control software functions properly and enables remote management of the system.

After commissioning was compete a set of experiments were performed with the system to investigate the effects of different activators on a zirconocene-catalyzed polymerization reaction of 1-hexene. Exotherm data was collected from the thermal camera and analysed using a heat balance to determine the activity of each activator. The exotherm data was then converted into catalytic productivity, normalized and scaled in preparation for neural network training.

The data from the various experiments, plotted as the average of normalized specific activity over the trials, is shown in Fig. 4. It is visible that certain activators were much more effective than others, with a maximum being seen while using (A2) aluminium chloride and comparable performance seen from (A3) boron trifluoride and (A4) sodium borohydride. (A1) Boron trichloride, (A5) antimony chloride and (A6) triethylamine had lower normalized specific activity. However, since (A6) triethylamine does not have an electron withdrawing group, it is unclear as to why the catalytic productivity was as high. As expected, (A9) phenylboronic acid had no quantifiable activity being the negative control. There was no observable clogging in the system as the monomer was rather dilute in the solvent, ensuring large quantities of polymer would not block the reactor. Between trials a small amount (~5 residence volumes) of toluene was rinsed through the system to further eliminate the possibility of polymer adhered to the reactor walls and prepare the reactor for the next trial.

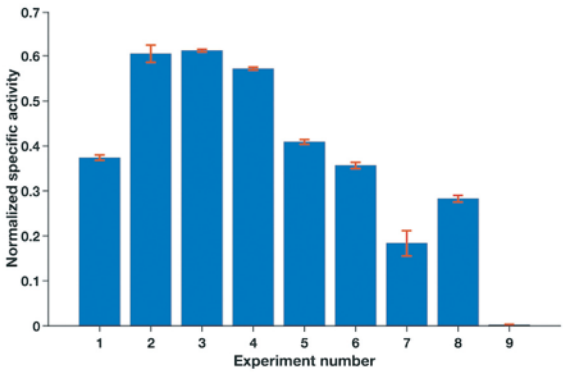

Fig. 4 Catalytic activity over the different experiments. Trial 1 used (A1) boron trichloride, 2 used (A2) aluminium chloride, 3 used (A3) boron trifluoride, 4 used (A4) sodium borohydride, 5 used (A5) antimony chloride, 6 used (A6) triethylamine, 7 used (A7) sodium tetrachloroaluminate, 8 used (A8) titanium chloride and 9 was a blank using (A9) phenylboronic acid.

Trends observed from this data include observations that borane compounds are generally active as co-catalysts, and it is anticipated based on the results and previous literature that borane compounds with other halides will exhibit a similar trend. Also, the electronegativity of the activator molecules plays an important role, and it can be seen both within the molecules and with counterions. Within the activator molecules it appears as though more highly electronegative functional groups enhance catalytic productivity. With counterions, a weaker coordination seems to be desirable. Finally, the size of the activator molecules also plays an important role as they have to fit within the active site of the catalyst, which does not seem as preferable with larger molecules and alkali metals.

Flow chemistry and microfluidics played important enabling roles in this study for two main reasons. Primarily flow chemistry allowed for efficient and quick experimentation. By performing the experiments continuously there is no down-time necessary to drain, clean and refill the reactor. Also the exotherm can be analysed over a period of time, enabling conclusions as to the standard deviation of catalytic productivity, further decreasing the time to actionable data. Microfluidics also plays a role in performing experiments quickly, but is particularly important for the miniaturization of the system and the ability to analyse the exotherm. In a larger batch systems, the details of the exotherm might be obscured by heat transport and non-homogeneous mixing, both parameters which are accounted for in microfluidic systems. Overall flow microsystems played an important role in being able to quickly and efficiently gather data regarding the catalytic polymerization reaction.

For the next part of the investigation nine different ANNs were trained using transfer learning and the results over the experimental space were observed. By using transfer learning and Bayesian regularization paired with normalization it was possible to largely eliminate the possible effects of overfitting, as the network generalized well between different input pairs. Also, the network architecture retains flexibility for future trials, involving new input and output pairs. Transfer learning training is much faster than training a network from scratch, enabling experimental results to be interpreted almost in real time. These results can be seen in Fig. 5 mapped over monomer and activator concentrations, with darker colours representing regions of lower activity. As expected (A1) boron trichloride, (A2) aluminium chloride, (A3) boron trifluoride, (A4) sodium borohydride, (A5) antimony chloride, and (A7) sodium tetrachloroaluminate all showed regions of preferable activity. In the case of (A1) boron trichloride, this predicted region is at low concentrations of activator and low concentrations of monomer. For (A2) aluminium chloride, the region is at high activator and low monomer concentrations. (A3) Boron trifluoride closely follows the behaviour of (A1) boron trichloride, as expected since they are both boron-based

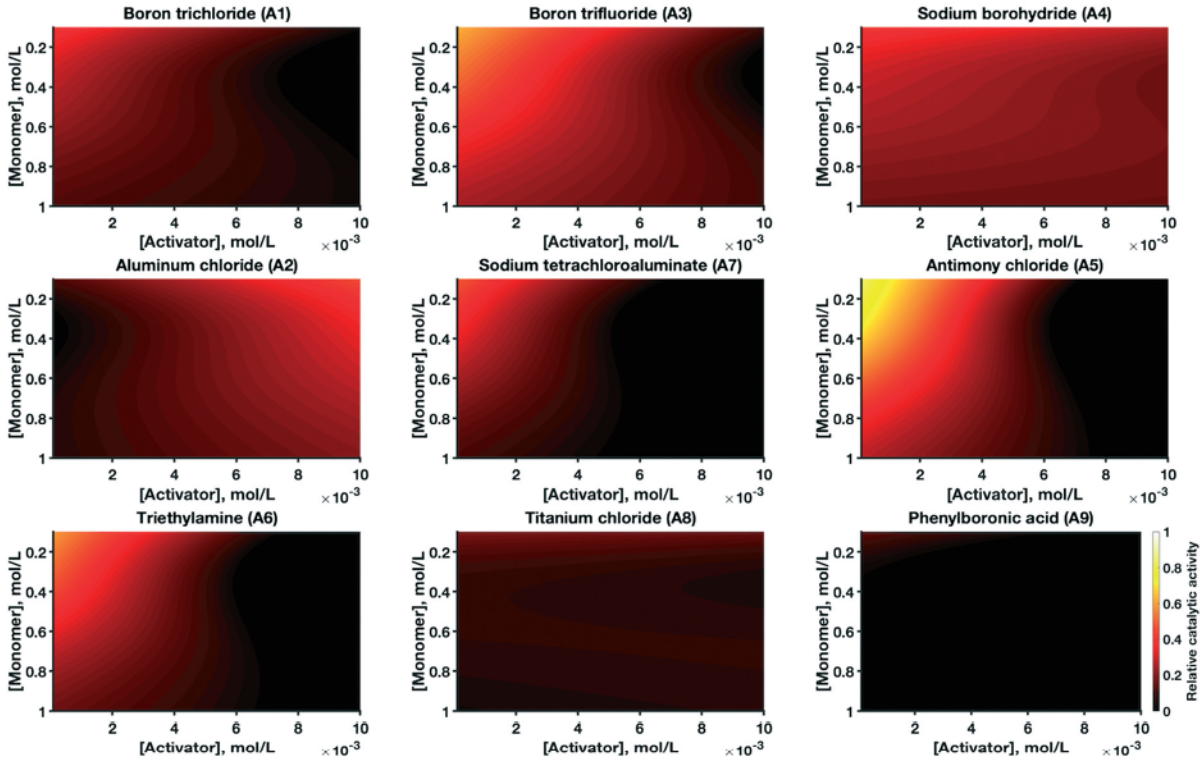

Fig. 5 Concentration response profiles for the various activators mapped over activator and monomer concentration ranges. Darker colours represent regions of lower catalytic activity while brighter colours represent higher activity.

compounds. (A4) Sodium borohydride shows a broad area of medium-high activity, with no clear maximum within the region investigated. (A5) In the case of antimony chloride a region of hypothesized preferential activity at low monomer and low activator concentrations, emerged as the strongest candidate. (A6) Triethylamine and (A7) sodium tetrachloroaluminate both showed regions of elevated activity with similar behaviour to (A5) antimony chloride, but not as highly active. (A8) Titanium chloride does not show a clear region of preferable activity. Finally, (A9) phenylboronic acid shows no activity, as would be expected for the negative control.

The entire study generated 60 mL of chemical waste, was performed in under two hours (neglecting glovebox time) and used around 150 watt-hours of electricity. All these figures are significantly decreased from a traditional study using batch mixed-tank reactors in a fume hood. For instance, 10 mL-to-10 L conventional reactors would produce two-to-four orders of magnitude more waste and require weeks-to-months of experiments to obtain the same information. Furthermore, the amount of catalyst used was also significantly decreased over traditional batch studies. Overall, the system and methodology presented have clear benefits both in terms of time to actionable data and the environmental footprint of catalytic discovery.

The μAIR-LAB system performed as expected, offering the ability to screen these different activators (A1–A9) quickly and efficiently. The results were interpreted using infrared thermography and a heat balance approach to quickly ascertain the catalytic productivity under different circumstances. The results were extended using transfer learning and machine intelligence to gather more information about the reaction space topology for these different activators. The system hints that in the future the speed and footprint of chemical studies can be further improved, including the implementation of droplet-based microfluidics.

The reactor design presented here is also easily extensible to other catalytic reactions where high-throughput flow-based microfluidics can be used. The small residence volume of the system along with good mixing characteristics allow for the ability to quickly screen catalysts, co-catalysts or other forms of exothermic reactions. Furthermore, the flexible nature of the microreactor enclosure with the hot-swappable rails enables quickly switching reactors in case of a failure mode (clogging, cracking, *etc.*) or to enable the investigation of different physics in the system. The infrared camera can also be swapped for a colour camera for studies involving chromatic indicators. The rails can be further modified to provide front, back or side illumination for photochemical studies. Finally, the entire system remains highly portable, enabling a decentralization of discovery from purpose-built laboratories.

Conclusions

A scalable, portable and automated microfluidic reactor laboratory (μAIR-LAB) was constructed into a Pelican® 1870 transport case using an aluminium framing internal

structure. The microreactor platform was paired with infrared thermography for exotherm analysis, pumps, manifolds and associated process support and control infrastructure. The system performed as expected and offers potential guidance for a future where homogeneous olefin catalysis research can be decoupled from large purpose-built and energy intensive laboratories.

An evaluation of the catalytic activity of nine different activators consumed two-to-four orders of magnitude less chemical waste, and it required hours of experiments compared with weeks-to-months using conventional laboratory-scale reactors. It was demonstrated that with boron activators moving from (**A1**) chloride to (**A3**) fluoride increased the catalytic productivity with low concentrations of activator providing good relative catalytic activity. (**A2**) Aluminium chloride however demonstrated the opposite behaviour, with the highest performance seen with higher concentrations. (**A4**) Sodium borohydride shows behaviour similar to the other boron compounds (**A1**, **A3**), hinting at how boron might interact with the active site of the catalyst. However, (**A7**) sodium tetrachloroaluminate showed virtually no activity at higher concentrations, due perhaps to the larger size of the molecule. (**A5**) Antimony chloride showed behaviour opposite to that of (**A2**) aluminium chloride, hinting at stronger inter-molecular interactions with the larger metal. Finally, the results help support that molecular size and electronegativity play an important role. Overall possible conclusions from this dataset include that borane compounds offer versatile performance, electron-withdrawing and steric considerations are important and counterions with a weaker coordination ability may enhance catalytic productivity. These conclusions and ranges of catalytic productivities obtained herein are largely consistent with previous works.

In the future, the system presented here could be used in a variety of application including and beyond exothermic polymerization catalysis. The modular nature of the box and the microreactor enclosure allow for the ability to include new analytical methods such as spectrometers or a benchtop NMR. The microreactor could be replaced with different architectures aimed towards other reactions. The entire system could be easily packed up and shipped to different labs for integrations with high frequency NMRs, synchrotrons or other unique and immovable spectroscopic instrumentation. Additionally, due to the compact size and low power requirements of the system it can be used to perform either experimentation or synthesis in remote areas, regulated labs with minimal space availability or in applications where quick deployment is necessary. For example, the system can be adapted for completely off-grid application such as the chemical testing in a war zone. Overall the ability to contain an autonomous research system with microfluidic reactors and spectroscopic equipment in a compact and portable environment allows for new and exciting applications in the field of chemical reaction engineering.

Conflicts of interest

There are no conflicts to declare.

Acknowledgements

This material is based upon work supported by the National Science Foundation under Grant Number CBET-1701393. Any opinions, findings, and conclusions or recommendations expressed in this material are those of the authors and do not necessarily reflect the views of the National Science Foundation.

Notes and references

1 T. J. Hutley and M. Ouederni, *Polyolefins—The History and Economic Impact*, 2016.
2 S. T. Knox and N. J. Warren, *React. Chem. Eng.*, 2020, **5**, 405–423.
3 V. Busico, *Macromol. Chem. Phys.*, 2007, **208**, 26–29.
4 E. A. Sanginov, A. N. Panin, S. L. Saratovskikh and N. M. Bravaya, *Polym. Sci., Ser. A*, 2006, **48**, 99–106.
5 A. Shamiri, M. Chakrabarti, S. Jahan, M. Hussain, W. Kaminsky, P. Aravind and W. Yehye, *Materials*, 2014, **7**, 5069–5108.
6 V. Sumerin and J. T. Ziegler-Natta, Catalyst and Preparation Thereof, *US Pat.*, 10,118,977 B2, 2018.
7 Y. Yu, R. Cipullo and C. Boisson, *ACS Catal.*, 2019, **9**, 3098–3103.
8 A. Vittoria, A. Meppelder, N. Friederichs, V. Busico and R. Cipullo, *ACS Catal.*, 2017, **7**, 4509–4518.
9 A. Vittoria, A. Meppelder, N. Friederichs, V. Busico and R. Cipullo, *ACS Catal.*, 2019, **10**, 644–651.
10 M. S. W. Chan, K. Vanka, C. C. Pye and T. Ziegler, *Organometallics*, 1999, **18**, 4624–4636.
11 J. W. Andzelm, A. E. Alvarado-Swaisgood, F. U. Axe, M. W. Doyle, G. Fitzgerald, C. M. Freeman, A. M. Gorman, J.-R. Hill, C. M. Kölmel, S. M. Levine, P. W. Saxe, K. Stark, L. Subramanian, M. A. van Daelen, E. Wimmer and J. M. Newsam, *Catal. Today*, 1999, **50**, 451–477.
12 P. Galli, G. Cecchin, J. C. Chadwick, D. Del Duca and G. Vecellio, *Metalorg. Catal. Synth. Polym., [Int. Symp.]*, 2011, 14–29.
13 E. Y. X. Chen and T. J. Marks, *Chem. Rev.*, 2000, **100**, 1391–1434.
14 H. S. Fogler, *Elements of Chemical Reaction Engineering*, 2016.
15 D. E. Fitzpatrick, C. Battilocchio and S. V. Ley, *ACS Cent. Sci.*, 2016, **2**, 131–138.
16 T. Junkers, *Macromol. Chem. Phys.*, 2017, **218**, 1–9.
17 S. Parkinson, N. S. Hondow, J. S. Conteh, R. A. Bourne and N. J. Warren, *React. Chem. Eng.*, 2019, **4**, 852–861.
18 J. J. Haven, J. Vandenbergh and T. Junkers, *Chem. Commun.*, 2015, **51**, 4611–4614.
19 C. Tonhauser, A. Natalello, H. Löwe and H. Frey, *Macromolecules*, 2012, **45**, 9551–9570.
20 B. Wenn, M. Conradi, A. D. Carreiras, D. M. Haddleton and T. Junkers, *Polym. Chem.*, 2014, **5**, 3053–3060.

21 K. Iida, T. Q. Chastek, K. L. Beers, K. A. Cavicchi, J. Chun and M. J. Fasolka, *Lab Chip*, 2009, **9**, 339–345.
22 F. Wurm, D. Wilms, J. Klos, H. Löwe and H. Frey, *Macromol. Chem. Phys.*, 2008, **209**, 1106–1114.
23 B. A. Rizkin, A. S. Shkolnik, N. J. Ferraro and R. L. Hartman, *Nat. Mach. Intell.*, 2020, **2**, 200–209.
24 A. Natalello, J. Morsbach, A. Friedel, A. Alkan, C. Tonhauser, A. H. E. Müller and H. Frey, *Org. Process Res. Dev.*, 2014, **18**, 1408–1412.
25 E. Baeten, S. Vanslambrouck, C. Jérôme, P. Lecomte and T. Junkers, *Eur. Polym. J.*, 2016, **80**, 208–218.
26 J. Vandenbergh, T. Tura, E. Baeten and T. Junkers, *J. Polym. Sci., Part A: Polym. Chem.*, 2014, **52**, 1263–1274.
27 A. Melker, B. P. Fors, C. J. Hawker and J. E. Poelma, *J. Polym. Sci., Part A: Polym. Chem.*, 2015, **53**, 2693–2698.
28 N. Micic, A. Young, J. Rosselgong and C. H. Hornung, *Processes*, 2014, **2**, 58–70.
29 J. Peng, C. Tian, L. Zhang, Z. Cheng and X. Zhu, *Polym. Chem.*, 2017, **8**, 1495–1506.
30 C. H. Hornung, C. Guerrero-Sanchez, M. Brasholz, S. Saubern, J. Chiefari, G. Moad, E. Rizzardo and S. H. Thang, *Org. Process Res. Dev.*, 2011, **15**, 593–601.
31 Y. Song, M. Shang, G. Li, Z. H. Luo and Y. Su, *AIChE J.*, 2018, **64**, 1828–1840.
32 Y. Su, Y. Song and L. Xiang, *Top. Curr. Chem.*, 2018, **376**, 44.
33 J. M. Asua, *Macromol. React. Eng.*, 2016, **10**, 311–323.
34 M. H. Reis, T. P. Varner and F. A. Leibfarth, *Macromolecules*, 2019, **52**, 3551–3557.
35 N. Corrigan, R. Manahan, Z. T. Lew, J. Yeow, J. Xu and C. Boyer, *Macromolecules*, 2018, **51**, 4553–4563.
36 N. Corrigan, L. Zhernakov, M. H. Hashim, J. Xu and C. Boyer, *React. Chem. Eng.*, 2019, **4**, 1216–1228.
37 G. J. M. Gruter, A. Graham, B. McKay and F. Gilardoni, *Macromol. Rapid Commun.*, 2003, **24**, 73–80.
38 D. D. Devore and R. M. Jenkins, *Comments Inorg. Chem.*, 2014, **34**, 17–41.
39 K. Sanderson, *Nature*, 2019, **568**, 577–579.
40 V. Busico, R. Pellecchia, F. Cutillo and R. Cipullo, *Macromol. Rapid Commun.*, 2009, **30**, 1697–1708.
41 P. Chammingkwan, M. Terano and T. Taniike, *ACS Comb. Sci.*, 2017, **19**, 331–342.
42 H. Zhang, V. Marin, M. W. M. Fijten and U. S. Schubert, *J. Polym. Sci., Part A: Polym. Chem.*, 2004, **42**, 1876–1885.
43 C. R. Becer, R. M. Paulus, R. Hoogenboom and U. S. Schubert, *J. Polym. Sci., Part A: Polym. Chem.*, 2006, **44**, 6202–6213.
44 A. Vittoria, A. Mingione, R. A. Abbate, R. Cipullo and V. Busico, *Ind. Eng. Chem. Res.*, 2019, **58**, 14729–14735.
45 M. Rubens, J. H. Vrijsen, J. Laun and T. Junkers, *Angew. Chem., Int. Ed.*, 2019, **58**, 3183–3187.
46 M. Rubens, J. Van Herck and T. Junkers, *ACS Macro Lett.*, 2019, **8**, 1437–1441.
47 A. Mannodi-Kanakkithodi, G. Pilania, T. D. Huan, T. Lookman and R. Ramprasad, *Sci. Rep.*, 2016, **6**, 1–10.
48 T. D. Huan, A. Mannodi-Kanakkithodi, C. Kim, V. Sharma, G. Pilania and R. Ramprasad, *Sci. Data*, 2016, **3**, 1–10.
49 C. Kim, A. Chandrasekaran, T. D. Huan, D. Das and R. Ramprasad, *J. Phys. Chem. C*, 2018, **122**, 17575–17585.
50 J. N. Kumar, Q. Li and Y. Jun, *MRS Commun.*, 2019, **9**, 537–544.
51 A. Nayak and S. K. Gupta, *Macromol. Theory Simul.*, 2004, **13**, 73–85.
52 S. Curteanu and F. Leon, *Int. J. Quantum Chem.*, 2008, **108**, 617–630.
53 W.-M. Chan and C. A. O. Nascimento, *J. Appl. Polym. Sci.*, 1994, **53**, 1277–1289.
54 B. A. Rizkin and R. L. Hartman, *Chem. Eng. Sci.*, 2019, **210**, 115224.
55 A. M. Alb and W. F. Reed, *Macromol. React. Eng.*, 2010, **4**, 470–485.
56 J. J. Haven and T. Junkers, *Eur. J. Org. Chem.*, 2017, **2017**, 6474–6482.
57 E. Frauendorfer, A. Wolf and W. D. Hergeth, *Chem. Eng. Technol.*, 2010, **33**, 1767–1778.
58 J. Yue, J. C. Schouten and T. Alexander Nijhuis, *Ind. Eng. Chem. Res.*, 2012, **51**, 14583–14609.
59 B. A. Rizkin, F. G. Popovic and R. L. Hartman, *J. Vac. Sci. Technol., A*, 2019, **37**, 050801.
60 F. H. Florenzano, R. Strelitzki and W. F. Reed, *Macromolecules*, 1998, **31**, 7226–7238.
61 T. McAfee, N. Leonardi, R. Montgomery, J. Siqueira, T. Zekoski, M. F. Drenski and W. F. Reed, *Macromolecules*, 2016, **49**, 7170–7183.
62 G. E. Fonseca, M. A. Dubé and A. Penlidis, *Macromol. React. Eng.*, 2009, **3**, 327–373.
63 I. S. De Buruaga, P. D. Armitage, J. R. Leiza and J. M. Asua, *Ind. Eng. Chem. Res.*, 1997, **36**, 4243–4254.
64 G. Fevotte, I. Barudio and J. Guillot, *Thermochim. Acta*, 1996, **289**, 223–242.
65 L. V. de la Rosa, E. D. Sudol, M. S. El-Aasser and A. Klein, *J. Polym. Sci., Part A: Polym. Chem.*, 1996, **34**, 461–473.
66 M. Esposito, C. Sayer and P. H. H. De Araújo, *Macromol. React. Eng.*, 2010, **4**, 682–690.
67 R. L. Hartman, J. R. Naber, S. L. Buchwald and K. F. Jensen, *Angew. Chem., Int. Ed.*, 2010, **49**, 899–903.
68 B. A. Rizkin, K. Popovich and R. L. Hartman, *Comput. Chem. Eng.*, 2019, **121**, 584–593.